THE MECHANISM OF LATEX PROTECTION AGAINST CHLORIDE INDUCED REBAR CORROSION

H. Justnes, Research Engineer (PhD),
The Cement and Concrete Research Institute at the Foundation for Scientific and Industrial Research, N-7034 Trondheim, NORWAY

J. Cantens (MSc) and J. Polet (MSc),
Department of Civil Engineering,
Katholieke Universiteit Leuven,
de Croylaan 2, B-3030 Heverlee, BELGIUM

ABSTRACT

The study was carried out in order to find out why some latexes perform vastly better than others in the chloride ingress test based on embedded rebars. The chloride profile in long time exposed samples were analysed. Furthermore, the conductivity and corrosion rate of embedded steel in different mortars were measured. The variables in the latter experiment were polymer dosage, polymer types, moisture level and chloride content. The best latex seemed to block chlorides completely from reaching the embedded rebar. In addition, this latex lead to the lowest conductivity, one of the key properties controling the corrosion rate.

Key-words: Latex, Polymer Cement Mortars, PCC, Chloride Ingress, Rebar Corrosion

1. INTRODUCTION

Latexes are often used in repair mortars for reinforced concrete suffering from chloride induced corrosion. Furthermore, latex may be added to mortar layers for protection of concrete exposed to chlorides (e.g. marine structures or bridge decks), or be added to the concrete for the most exposed parts of a structure (e.g. bridge pilars) at the construction site, as discussed by Justnes et al /1/.

Recently, an acrylic latex (ACR) has been developed /2/ that when used in PCC gives an excellent performance against chloride induced corrosion /1, 3/ compared with commonly used latexes like for instance SBR (Styrene-Butadiene Rubber), as shown in Table 1. The test is an accelerated impressed current test which measures the time before the current increases in a circuit between the rebar embedded in the mortar (+) and a steel plate (-) placed in the same sea water tank as the mortar, similar to the method used by the Federal Highway Administration, USA /4/. The increase in current is attributed to the chlorides reaching the rebar and the consecutive penetration of the protective oxide layer on the rebar, justifying the method being a "chloride ingress" test. The object of this study was to elaborate why PCC based on the ACR-latex perform

vastly better than the SBR analogue in this test. Do the latex block the chlorides completely, or is the reason a corrosion inhibiting effect? Thus, the chloride profiles in some old cylindres from the chloride ingress test based on embedded rebars /1/ were analysed. In addition, the corrosion rate of embedded steel in mortars with different latexes, dosages of latexes, chloride levels and moisture conditions were measured in order to find an answer.

Table 1. Time (days) before current rise in the chloride ingress test /4/ for mortar with w/c = 0.40 and different types and dosages of latex /1/.

Latex	0 %	5 %	10 %	15 %	20 %
ACR	105±35	350±2	651±7	783±8	777±1
SBR	105±35	125±0	118±28	103±7	90±5

2. EXPERIMENTAL

2.1 Chloride ingress

The chloride profile of mortar with w/c = 0.55 and 10, 15 and 20 % ACR (two parallels) from cylindres with embedded rebar after 1 year in the chloride ingress test with impressed current (5 V DC) were analysed. The cylindres were taken out of the test before a current increase was detected (terminated experiment), and stored at about 20°C and 45 % R.H. for another year prior to the chloride analyses.

Figure 1a shows how samples were taken from the cylindres. The cylindres were first split in two, and with a diamond saw a slice of about 2 cm thickness was cut from one of the halfes (No. 1). Out of this slice, three radials were cut as shown in figure 1b. Each of these radials was cut in 4-6 smaller pieces. For every piece, the distance from its center to the cylinder surface was registrated and the chloride content was measured by Volhard's titration of the acid extract of the crushed material.

The two remaining sawed cross-sections (pieces no. 2 and 3) were each sprayed with two different chloride indicators; a) 0.1 % sodium fluorescein solution followed by a 0.1 N $AgNO_3$, and b) 1 % silver nitrate solution followed by a 5 % potassium chromate, K_2CrO_4, solution. This will reveal the cross-sectional profile of a certain chloride content in the mortar, with a light part being rich in chlorides and a dark part with a lower chloride content. In addition, the other half of the cylinder (no. 4) was sprayed with indicator a) and b) in order to detect the longitudinal profile of the same chloride content. The object was to estimate the chloride content at the point of colour change for the two indicators, utilizing the chloride ingress profiles from the analyses. Another purpose was to evaluate the usefulness of the two chloride indicators.

The chloride content of two cylindres from mortar with composition; 5 % ACR and w/c = 0.55, were analysed for the chloride content close to the rebar. These cylindres whithstood the chloride ingress test for 35±1 days before corrosion was detected, compared with 3±1 days for the reference mortar with 0 % polymer and w/c = 0.55 /1/. Two mortar samples were taken from both cylinders close to the rebar. The object was to find which chloride level the corrosion started at.

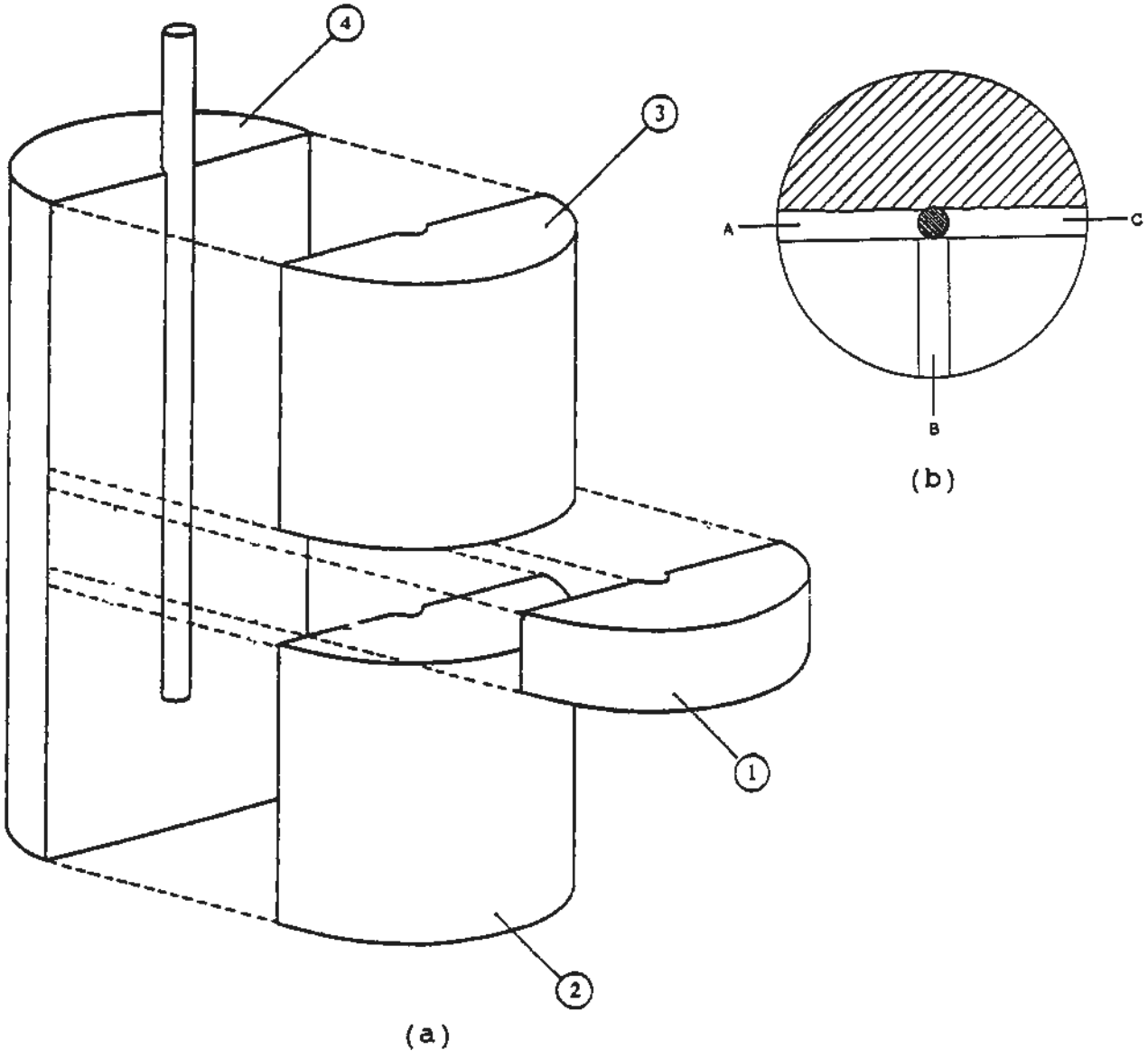

FIG. 1. (a) Location of the different samples for chloride measurements in a cylinder. (b) Position of the radials cut from sample no. 1.

2.2 Corrosion rate

The instantaneous corrosion rate of a metal in a defined environment may be determined by the electrochemical method polarization resistance measurements.

2.2.1 Principle of polarization resistance measurements

In 1957, Stern et al /5, 6/ published their first paper on the relationship between a small step of potential, ΔE, applied to the corrosion potential, E_{Corr}, of a metal environment system and the resulting current, I. They defined the polarization resistance, R_p, as;

$$R_p = \left(\frac{\Delta E}{\Delta I} \right)_{\Delta E=0} \qquad (1)$$

Using the Stern-Geary equation, the instantaneous corrosion rate, i_{Corr}, can be computed as;

$$i_{Corr} = \frac{B}{R_p} \qquad (2)$$

where

$$B = \frac{(\beta_a \cdot \beta_c)}{2.3 \cdot (\beta_a + \beta_c)} \qquad (3)$$

The coefficients β_a and β_c are the tafel slopes, and correspond to the kinetic coefficients of the anodic and cathodic reactions of the corroding system, respectively /5, 6/.

Most authors assume a B-value of 26 mV /7/ for cement mortars. This value has been proven to be in good agreement with gravimetrical experiments where the weight loss due to corrosion has been measured directly on embedded electrodes. However, there is still some discussion about the B value /8, 9/, and the value may vary between 13 and 52 mV.

2.2.2 Procedure and equipment for polarization resistance measurements

The measurement of the polarization resistance is based on a potentiodynamic linear polarization method using a Corrovit instrument and a reference electrode (Radiometer K401 Calomel Electrode). The corrosion potential of the working electrode, E_{Corr}, versus the reference electrode is measured first by the Corrovite apparatus. Then the reference electrode is placed on the mortar surface (Fig. 2a) as close as possible to the working electrode

(Fig. 2b), while a constant, controled potential is imposed on the working electrode. This potential is adjustable by means of an incorporated voltage offset circuit and is put equal in magnitude, but opposite in sign, to the corrosion potential. At this moment, no current flows through the cell. The controled potential is then swept between E_{Corr}+12,5 mV and E_{Corr}-12,5 mV at a sweep rate of 0.2 mV/sec. The signal is connected to the X-axis of an XY-plotter. The resulting current through the cell is measured as Y-values by a current measuring amplifier and plotted as a curve in a XY-diagram.

In order to measure the corrosion rate, i_{Corr}, the tangent to the polarization curve (Fig. 3) is drawn as a straight line through the origin of the plot. R_p is measured as the slope of this line and computed by the formula in equation (1). The corrosion rate is then;

$$i_{Corr} = \frac{0.026}{R_p \cdot 6.50} \cdot 10^6 \quad [\mu A/cm^2] \qquad (4)$$

where 6.50 is the exposed area of the electrode in cm^2.

Four basic mixes were studied by the above method; 5 % ACR, 10 % ACR, 10 % SBR and a reference mortar with no polymer addition, all with w/c-ratio 0.55. The polymer content refers to a volume replacement of the cement paste (cement + water) by solid polymer, leaving both the binder volume and the w/c-ratio constant. The composition of the reference mortar was 4000 g P30-cement (Norcem A/S), 4000 g sand (0-0.5 mm), 2000 g sand (0.5-1 mm), 2000 g sand (1-2 mm), 4000 g sand (2-4 mm), 800 g calcite filler and 2200 g water. The sand was delivered dry from Svelvik Sand A/S, Kilemoen, Hønefoss, while the filler was supplied by Franzefoss Bruk A/S. All the mortars had an air content below 5 vol%. For each basic mix, one was made without and one with 2 % salt added to the mixing water, making a total of 8 mixes. From each of the 8 mixes, 6 prisms were cast with two incorporated electrodes (ϕ = 6 mm). These electrodes were taped, leaving an uncovered part of 33 mm from the bottom of the electrode, corresponding to an area of 6.5 cm^2 (Fig. 2b). The whole uncovered area of the electrode was embedded in the mortar. Three prisms from each mix were cured according to a "dry" and a "wet" scheme prior to the measurements: "Dry"; 1 day in molds covered with plastic film, 27 days at 50 % R.H. and until 2 or 3 months age at 90 % R.H. "Wet"; same as "dry" until 28 days age, but stored in water instead of 90 % R.H. The prisms containing salt and cured according to the "wet" scheme were stored in a 2 % salt solution in order to prevent leaching of salt from the prisms.

2.3 Electrical resistance

The electrical resistance of the specimens described in section 2.2.2 was also measured every time the polarization measurement was carried out. For this purpose, a Wayne Kerr Automatic Component Bridge B 605 was used. In order to avoid hydrolysis effects, the resistance was measured in A.C. with a frequency of 1 kHz.

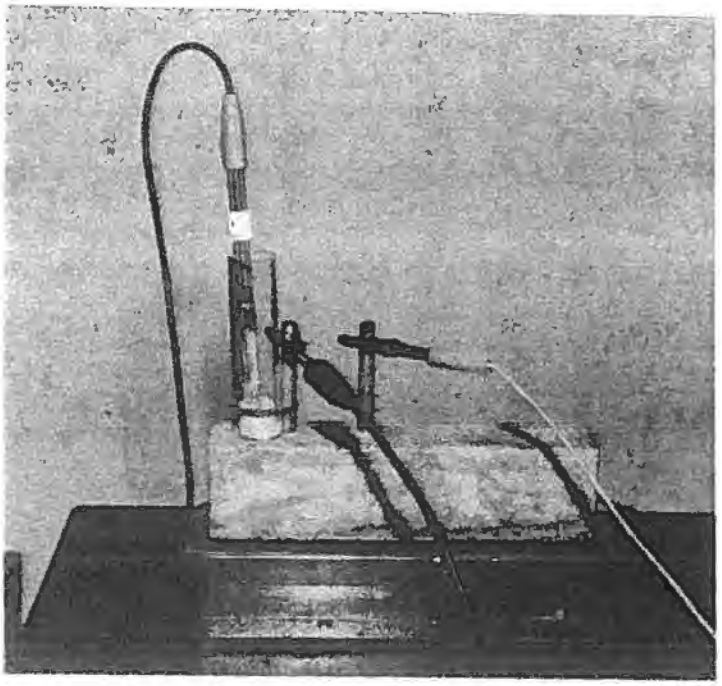

(a)

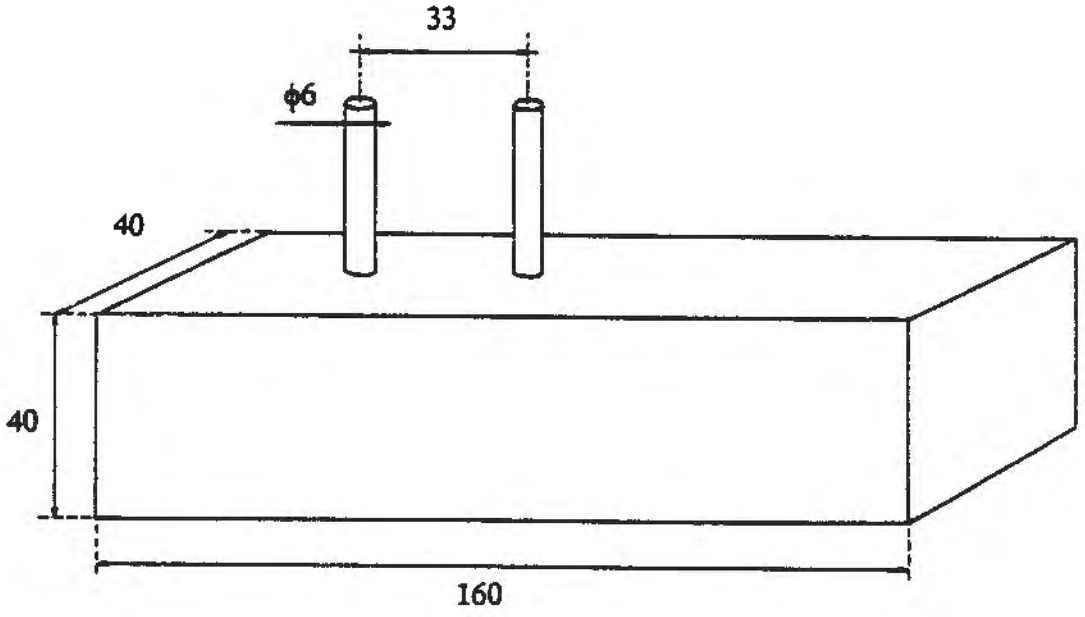

(b)

Fig. 2. (a) Close-up of a prism for the polarization resistance measurement with the reference electrode mounted. (b) Dimensions of the specimen for polarization resistance measurements.

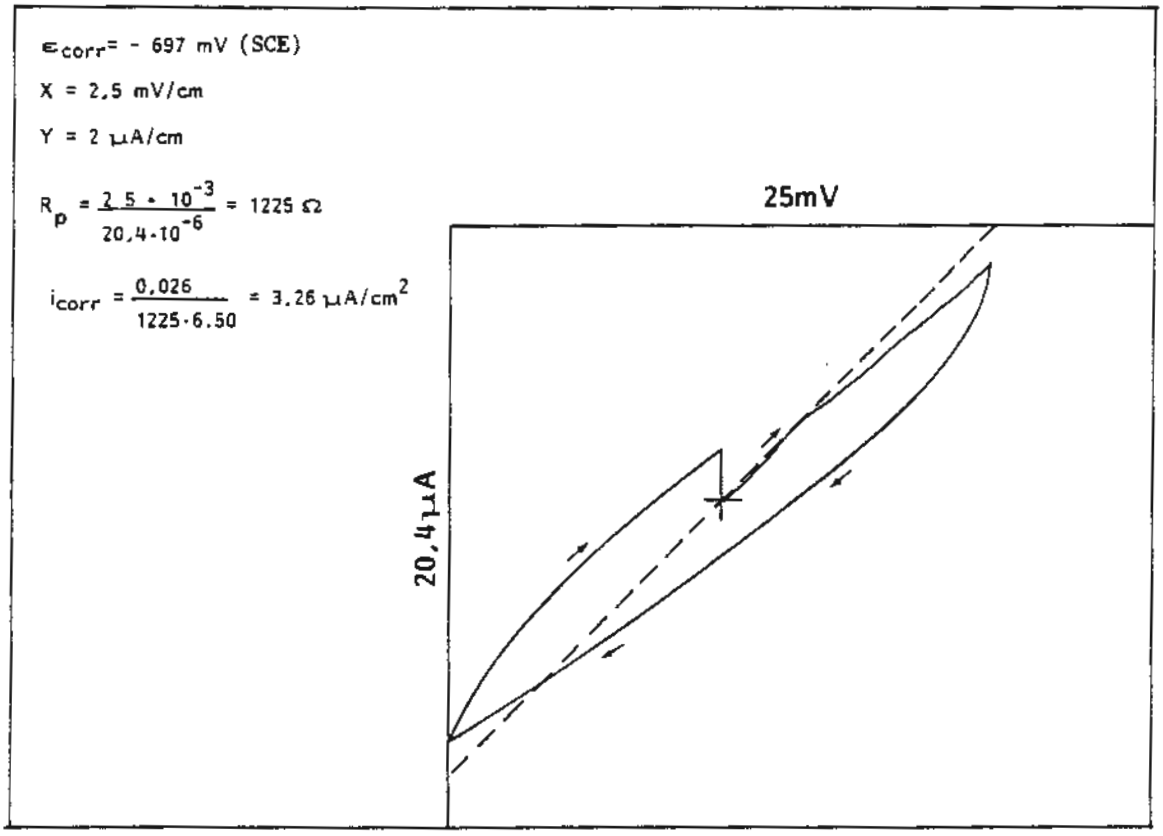

Fig. 3. An example of a polarization curve with the determination of i_{Corr}.

2.4 Degree of hydration

The degree of hydration for the cement in the 2 year old mortar cylindres with 10, 15 and 20 % ACR were measured for a piece broken from the lower part of the cylinder part no. 4 (see figure 1a). The piece were crushed into particles of about 1 mm size, which then were dried until constant weight at 105°C. A sample of about 40 g was then burned at 950°C for 24 h. It was assumed that the recorded weight loss is due to burned polymer, decomposed water from the CSH-gel and CO_2 from the calcite filler. The degree of hydration may then be calculated by mass balances from the weight difference before and after burning as shown by Øye /10/. The purpose was to investigate if increased latex additions would lead to a decreased degree of hydration even at long terms, leading to a more permeable cement paste.

3. RESULTS

3.1 Chloride ingress

The chloride profile of a two year old cylinder with 10 % ACR is shown as an example in figure 4a. The indicator profiles of the same cylinder are exhibited in figure 4b.

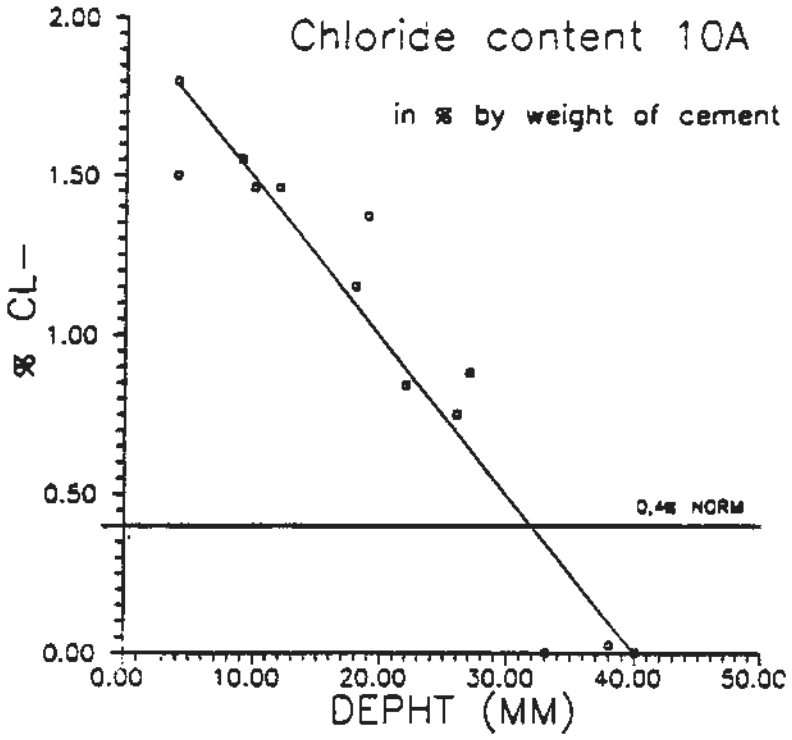

(a)

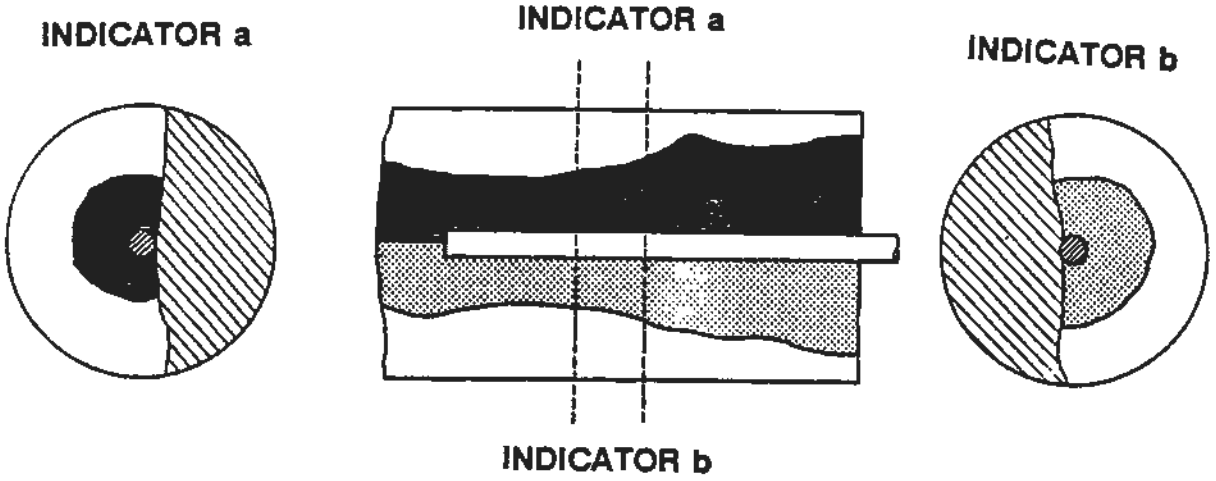

(b)

Fig. 4. (a) The chloride profile for one of the cylinders with 10 % ACR. (b) Indicator profiles for one of the cylinders with 10 % ACR.

The chloride profiles of all the cylinders were fitted by linear regression to the line; Cl^- % = a + b•Depth (mm), and the factors a and b are given in Table 2 together with the correlation factor for all the lines. See the drawn line in Fig. 4a.

Table 2. The parameters from the linear regression analyses of radial chloride profiles from mortar cylinders with different dosages of ACR latex.

ACR dosage	Factor a	Factor b	Linear regression coeff., r^2
10 %	1.94±0.08	-0.050±0.000	0.95±0.02
15 %	1.97±0.08	-0.054±0.000	0.96±0.02
20 %	2.56±0.06	-0.072±0.003	0.96±0.02

The linear relations in Table 2 were used when the chloride content at which the indicator a and b changed colour should be determined. The average distance from the surface to the colour change were determined for all the 8 cylindres between the two dotted lines shown in the middle of Fig. 4b. The result for both indicator a and b was a colour change at a chloride content of 0.8±0.1 % Cl^- of the cement weight.

The average chloride level in the failed cylinders with 5 % ACR and w/c = 0.55 was 1.02±0.04 % Cl^- of the cement weight close to the slightly corroded rebar.

3.2 Corrosion rate

The corrosion rate and corrosion potential of iron embedded in mortars with different dosages and types of latexes after 2 and 3 months curing according to two different schedules, and with and without salt additions, are given in Tables 3 and 4, respectively.

3.3 Electrical resistance

The electrical resistance between the two iron pieces embedded in mortars with different dosages and types of latexes after 2 and 3 months curing curing according to two different schedules (wet and dry), and with and without salt additions, are presented in Table 5 and 6, respectively. The corresponding resistivities, as calculated in section 4, are given as well.

3.4 Degree of hydration

The degree of hydration for the 2 year old mortars with 10, 15 and 20 % ACR and w/c = 0.40 were 78±4, 73±1 and 65±2 %, respectively.

Table 3. Results from polarization resistance measurements after 2 months curing according to two different schedules (dry and wet) for different polymer modified mortars with and without intermixed salt.

	Dry	Wet	Dry/salt	Wet/salt
Reference E_{Corr} (mV)	-238±78	-460±182	-386±110	-550±67
I_{Corr} ($\mu A/cm^2$)	0.13±0.05	1.6±0.9	0.6±0.7	1.6±0.4
5 % ACR E_{Corr} (mV)	-156±13	-173±50	-477±9	-496±85
I_{Corr} ($\mu A/cm^2$)	0.04±0.01	0.24±0.13	0.43±0.19	0.53±0.11
10 % ACR E_{Corr} (mV)	-155±22	-304±104	-413±37	-393±50
I_{Corr} ($\mu A/cm^2$)	0.06±0.01	0.16±0.08	0.24±0.10	0.31±0.18
10 % SBR E_{Corr} (mV)	-360±156	-331±132	-415±13	-412±53
I_{Corr} ($\mu A/cm^2$)	0.3±0.3	0.16±0.12	0.28±0.03	0.27±0.08

4. DISCUSSION

4.1 Factors affecting corrosion of rebars

The corrosion of rebars embedded in mortars or concrete may be divided into corrosion initiation and corrosion propagation.

4.1.1 Corrosion initiation

The high pH-level (12.6-13.3) of mortar and concrete leads to a protective oxide layer on embedded steel hindering the initiation of corrosion. Thus, corrosion will only start when either the pH-level is reduced (e.g. by carbonation) or the oxide layer is destroyed (e.g. by chlorides). In the case of chloride initiated corrosion, the main controling parameter is the Cl^-/OH^--ratio in the pore water next to the rebar. At pH = 13.00, corrosion may be initiated when the Cl^- concentration is 37 mmole/ℓ or 1310 mg/ℓ /11/. When chlorides are analyzed in concrete, the result is often presented as Cl^-/cement weight. The concentration in the pore water, however, depend on the amount bonded as Friedel's salt (about 60 % of total Cl^- for a P30-sement /12/) in the matrix. The concentration of chlorides next to the corroded rebars in the mortars with 5% ACR from the chloride ingress test was 1% Cl^- /cement weight. Thus, some of the mortars for the corrosion rate measurements were added 2 % NaCl to the mix water in order to initiate corrosion.

Table 4. Results from polarization resistance measurements after 3 months curing according to two different schedules (dry and wet) for different polymer modified mortars with and without intermixed salt.

	Dry	Wet	Dry/salt	Wet/salt
Reference E_{Corr} (mV)	-494±29	-442±58	-404±45	-533±80
I_{Corr} ($\mu A/cm^2$)	1.5±1.2	0.7±0.2	0.37±0.06	1.2±1.1
5 % ACR E_{Corr} (mV)	-176±25	-310±154	-426±21	-527±17
I_{Corr} ($\mu A/cm^2$)	0.04±0.01	0.3±0.2	0.24±0.09	0.48±0.07
10 % ACR E_{Corr} (mV)	-187±41	-535±66	-367±21	-497±26
I_{Corr} ($\mu A/cm^2$)	0.06±0.02	0.23±0.13	0.14±0.01	0.45±0.11
10 % SBR E_{Corr} (mV)	-395±42	-246±6	-365±47	-536±41
I_{Corr} ($\mu A/cm^2$)	0.15±0.09	0.15±0.06	0.16±0.04	0.59±0.17

4.1.2 Corrosion propagation

Once initiated, the rate of corrosion depends on 1) oxygen permeability, 2) moisture content, 3) electrical resistivity of the mortar and 4) cathode/anode-ratio of the rebar. Oxygen supply is usually rate limiting, since there is a direct proportionality beteen the amount of corroded metal released at the anodic site (oxidation process) and the amount of oxygen consumed at the cathodic sites (reduction process). The efficiency of the cathodic area is dependent on the electrical resistivity (see Tables 5 and 6) of the mortar; high electrical resistivity give a relatively low corrosion rate and vice versa.

Note that the permeability of the mortar not only is influencing the rate of corrosion, but is determining the time elapsed before the critical chloride level for corrosion initiation is reached at the rebar when the chlorides come from external sources (e.g. sea water).

Be aware that the lower permeability in latex modified mortar and concrete due to film formation of polymer in the pore system, may be counteracted by the lower degree of hydration, and thereby higher content of capillary pores, for cement with increasing dosages of polymer as observed in section 3.4. The inferior performance of PCC with 20 % ACR (65 % hydration) compared with 15 % ACR (73 % hydration), as seen in Table 1, may be due to the counteraction of a more permeable cement paste. However, the net result is in general still a lower permeability for latex modified mortar compared with mortars without polymer additions.

Table 5. The electrical resistance (upper), R (kΩ), and resistivity (lower), ϱ (Ω•m), for some polymer modified mortars after 2 months curing.

	Dry	Wet	Dry/salt	Wet/salt
Reference	3.4±1.5 35±15	1.05±0.03 11±0	2.0±0.6 20±6	0.94±0.05 9±0
5 % ACR	6.6±0.8 68±8	1.15±0.01 13±0	3.38±0.09 36±1	1.0±0.2 11±2
10 % ACR	9.5±0.9 99±89	1.27±0.07 13±1	4.3±0.4 44±4	0.93±0.12 9±1
10 % SBR	4.2±0.5 44±5	1.01±0.02 11±0	2.50±0.02 20±0	0.90±0.03 9±0

Table 6. The electrical resistance (upper), R (kΩ), and resistivity (lower), ϱ (Ω•m), for some polymer modified mortars after 3 months curing.

	Dry	Wet	Dry/salt	Wet/salt
Reference	4.0±0.6 41±6	1.30±0.03 14±0	2.5±0.8 25±8	1.06±0.07 11±1
5 % ACR	8.1±1.0 85±10	1.36±0.10 14±1	4.2±0.3 44±3	1.1±0.3 13±3
10 % ACR	11.1±0.8 115±8	1.61±0.08 16±1	4.9±0.4 52±4	1.05±0.13 11±1
10 % SBR	5.1±0.6 52±6	1.32±0.06 14±1	2.89±0.13 30±1	1.18±0.08 13±1

4.2 The mechanism of latex protection against chloride induced rebar corrosion

The results in Table 1 reveal that mortar based on the acrylic latex ACR perform vastly better than mortar based on styrene-butadiene rubber (SBR) latex in the chloride ingress test when the concept of both constant w/c-ratio and binder volume is used in the comparison. The chloride ingress test is described in detail elsewhere /1/, but it should be stressed that the mortar cylindres with embedded rebars are immersed in sea water. The chloride diffusion is accelerated by an impressed current from a 5 V D.C. set up between the rebar (+) and a metal sheet (-) in the sea water. The current flowing through the mortar is detected, and a sharp rise in the current is a criterion for chloride penetration to the rebar (i.e. initiated corrosion).

The reason why the SBR additions are hardly effective compared with the reference mortar (Table 1), is probably due to a partly re-emulsification of the polymer film when the mortar cylindres are placed for such a long time in water. The decreasing efficiency with increasing SBR dosage might be due to a decreased degree of hydration of cement, and thus increasing capillar porosity.

The ACR additions are increasingly effective with increasing dosages until 15 %. At 20 % the adverse effect of decreased cement hydration has overcome the positive effect of the polymer film. The ACR is a polymer that has been designed with "chemical anchors" /2/ leading to polymer films that can not reemulsify, and a possible explanation for the better performance than SBR may be that the polymer is much more effective in blocking the chlorides from entering the mortar. This seems to be the case from the results in Fig. 4 and Table 2.

Another possible explanation could be that the ACR polymer exhibits inhibiting properties against rebar corrosion. The answer is found from the results of the polarization resistance measurements as discussed below.

Alonso and Andrade /13/ have related the values of i_{Corr} to the corrosion state in concrete. An i_{Corr} < 0.1-0.2 $\mu A/cm^2$ indicate negligible corrosion, while greater values means active corrosion. In terms of service life, an i_{Corr} > 1 $\mu A/cm^2$ indicate important corrosion, while an i_{Corr} > 10 $\mu A/cm^2$ is severe corrosion. In this study, samples with i_{Corr} > 0.1 $\mu A/cm^2$ were classified as active. For active samples, the corrosion potential, E_{Corr}, was always < -200 mV.

The results in Tables 3 and 4 reveal two general trends; 1) the corrosion rate is greater in "wet" samples than in "dry" (90 % R.H.) and 2) the corrosion rate is greater in samples with salt additions than in those without. There are only a few exceptions from these tendencies.

The only passive samples are those with 5 % ACR and "dry" without salt after both 2 and 3 months curing and the same sample "wet" after 2 months curing only. In addition, the 10 % ACR samples, "dry" and without salt are passive after both 2 and 3 months curing. An explanation can be the particular high resistivity for these "dry" samples, as shown in Tables 5 and 6 and discussed in the next section.

The corrosion rates for the 10 % SBR samples are all nearly equal to the rates for the 10 % ACR samples, with the exception of the "dry" samples without salt additions. Thus, the conclusion is that the ACR-polymer does not inhibit corrosion chemically.

4.3 Electrical resistance and resistivity

The measured electrical resistance, R_{meas}, is converted to the material constant resistivity, ϱ, by the simple formula;

$$\varrho = R_{meas} \cdot A / \ell \qquad (5)$$

where A is the area of half the cylindric electrode = $\pi \cdot r \cdot h$ = 311 mm^2 and ℓ is the average distance (30 mm) between the electrode surfaces. Thus, the electrical resistances (kΩ) should be multiplied by a factor of 10.37 in order to convert to resistivity (Ω•m). Both values are listed in Table 5 and 6.

Brian and Alan /14/ determined the resistivity of cement mortars with w/c = 0.45 and 6 % air content after 45 days curing (3/11 days wet and dry cycle) to 91 Ω•m. When 2 % $CaCl_2$ was added to the same mortar during mixing, the resistivity dropped to 60 Ω•m at the same age and conditioning. Comparing these values with the reference mortar in the "dry" state after 2 months curing without (35 Ω•m) and with (20 Ω•m) 2 % NaCl addition from this study, the somewhat larger percentual drop in resistivity due to salt addition might be due to smaller ion Na^+ compared with Ca^{2+} or a higher ion content pr unit weight. The lower absolute value is probably due to the higher w/c-ratio (0.55) in this case (i.e. higher permeability).

The resistivity is an important factor for corrosion rate, and Brian and Alan /14/ estimate 100 Ω•m as a critical limit for corrosion to take place. The only mix with such a high resistivity, is the mortar with 10 % ACR in the dry state after 2 (99 Ω•m) and 3 months (115 Ω•m) curing. However, note that a low resistivity does not necessarily mean a transportation of chloride ions, since the charge may be transported by the much smaller (i.e. more mobile) hydroxide ions. The validity of this statement is supported by the relatively equal resistivity for samples with and without salt additions when they both are wet.

The much higher resistivity of the ACR modified mortars compared both with SBR modified samples and the reference mortars at 90 % R.H., indicates that the ACR latex will give the best protection against rebar corrosion when used in for instance repair mortars.

4.4 Application of chloride indicators

The chloride indicators a) and b) described in section 2.1 are not widely used, but indicator a) is described in the Japanese norm UNI 7928 and used to measure a "chloride penetration depth" /14/. The chloride resistance of different samples, exposed to the same chloride containing environment, might be compared by splitting them and spraying the fracture surfaces by the indicator.

However, unlike the phenolphtalein indicator for the carbonation test which change colour due to the pH-level, both chloride indicators rely on a chemical reaction consuming chlorides;

$$Ag^+ + Cl^- = AgCl\ (s) \qquad (6)$$

forming the white precipitate silver chloride. For indicator a), the excess silver will react with the hydroxide ions to form the dark brown precipitate silver oxide;

$$2\ Ag^{+} + 2\ OH^{-} = Ag_2O\ (s) + H_2O \qquad (7)$$

The sodium fluorescein is used in order to enhance the contrast. In indicator b), the silver nitrate spraying is followed by the application of potassium chromate, reacting with free silver to form insoluble, reddish brown silver chromate;

$$2\ Ag^{+} + CrO_4^{2-} = Ag_2CrO_4\ (s) \qquad (8)$$

It follows from reaction (6) that if more silver nitrate is applied, the Cl^- concentration for colour change will be shifted to a higher value. In other words, the method is operator dependent, and great care has to be taken in order to apply equal amounts of indicator each time. However, if the chloride profile is steep, as in Fig. 4a, the problem might not appear.

In this study, indicator a) seemed to give a better contrast than indicator b). The method is only recommended for quick comparisons.

5. CONCLUSION

The reason why mortars based on the acrylic latex (ACR) perform so well in the chloride ingress test compared with both mortars based on styren-butadiene rubber (SBR) latex and reference mortars without latex additions, is that it effectively hinder chlorides from reaching the rebar. No inhibiting effect against rebar corrosion has been revealed, but the ACR latex leads to an increased resistivity of the mortar at 90 % R.H., which in turn may cause a slower corrosion rate for embedded rebars.

Acknowledgement. The study results from a student exchange program between "the Katholieke Universiteit van Leuven" and "Norges Tekniske Høgskole i Trondheim". We would like to thank Prof. D. van Gemert, Belgium, and Prof. E. J. Sellevold, Norway, for making this exchange possible.

6. REFERENCES

/1/ Justnes, H., Øye, B.A. and Dennington, S.P.: "Protecting Concrete Against Chloride Ingress by Latex Additions". The conference "The Protection of Concrete", Dundee, 11-13 Sept. 1990, pp. 751-763

/2/ Justnes, H. and Dennington, S.P.: "Designing Latex for Cement and Concrete", Nordic Concrete Research, Publication No. 7 (1988), pp. 188-206.

/3/ Justnes, H. and Øye, B.A.: "Protecting Concrete against Chloride Ingress by Latex Additions". The 6th International Congress on Polymers in Concrete, Shanghai, China, Sept. 24-27, 1990, pp. 261-267

/4/ Brown, R.P. and Kessler, R.J.: "An Accelerated Laboratory Method for Corrosion Testing of Reinforced Concrete Using Impressed Current", Florida Department of Transportation, Office Materials and Research, Report No. Florida 206, October 1987, 26 pp.

/5/ Stern, M. an Geary, A.L., J. Electrochemical Society, Vol. 104, 1957, pp. 56-63

/6/ Stern, M. and Weisert, E.D.: "Experimental Observations on the Relation between Polarization Resistance and Corrosion Rate", Proceedings ASTM, Vol. 59, 1959, pp. 1280-1291.

/7/ Page, C.L. and Havdahl, J.: "Electrochemical Monitoring of Corrosion of Steel in Microsilica Cement Pastes", Materiaux et Constructions, 1985, No. 1, pp. 41-47.

/8/ Macias, A. and Andrade, C.: "Accuracy of Different Electrochemical Laboratory Techniques for Evaluating Corrosion Rates of Galvanized Reinforcements", Proceedings of the Fourth International Conference on Durability of Materials and Components, Singapore, 1987, pp. 516-522

/9/ Andrade, C., Castelo, V., Alonso, C. and Gonzales, J.A.: "The Determination of the Corrosion Rate of Steel Embedded in Concrete by the Polarization Resistance and AC Impedance Methods", Corrosion Effects of Stray Currents and the Techniques for Evaluating Corrosion of Rebars in Concrete, ASTM STP 906, V. Chaker (Ed.), ASTM, Philadelphia, USA, 1986, pp. 43-63

/10/ Øye, B.A.: "Repair Systems for Concrete - Polymer Cement Mortars. An Evaluation of Some Polymer Systems", PhD Thesis No. 57, 1989, Department of Inorganic Chemistry, the Norwegian Institute of Technology, Trondheim, Norway

/11/ Uhlig, H.H.: "The Corrosion Handbook". John Wiley & Sons, New York, 1955.

/12/ Gautefall, O. and Havdahl, J.: "Effect of Condensed Silica Fume on the Mechanism of Chloride Diffusion into Hardened Cement Paste", Proc. 3rd Int. Conf. Fly Ash, Silica Fume, Slag and Natural Pozzolans in Concrete, Trondheim, Norway, 1989, ACI SP 114-41 (Ed. V.M. Malhotra), pp. 849-860

/13/ Alonso, C. and Andrade, C.: "Effect of Nitrite as a Corrosion Inhibitor in Contaminated and Chloride-Free Carbonated Mortars", ACI Materials Journal, Vol. 87, No. 2, March-April, 1990, p. 131.

/14/ Ohama, Y., Sato, Y. and Nagao, H.: "Improvements in Watertightness and Resistance to Chloride Ion Penetration of Concrete by Silane Impregnation", Proceedings of the Fourth International Conference on Durability of Building Materials and Components, Singapore, 1987, pp. 295-302.